

第六届粒子物理天问论坛



Light single-gluon hybrid states with various
exotic quantum numbers

Wei-Han Tan

Southeast University

Collaborator: Niu Su, Hua-Xing Chen, Shi-Lin Zhu, Wei Chen





Outline

- **Introduction**
- **Method of the QCD sum rules**
- **Numerical analyses**
- **Decay behavior**
- **Summary**

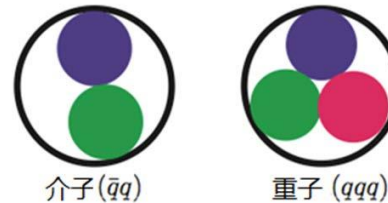


Outline

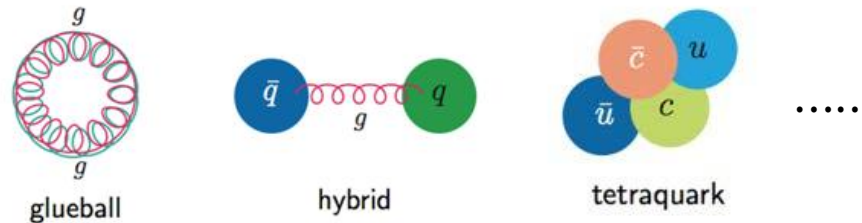
- **Introduction**
- Method of the QCD sum rules
- Numerical analyses
- Decay behavior
- Summary

Introduction

- Traditional quark model



- Exotic hadron: **hybrid state**, glueball, tetraquark, etc.



- Exotic spin-parity quantum numbers

$$0^{--}, 0^{+-}, 1^{-+}, 2^{+-}$$

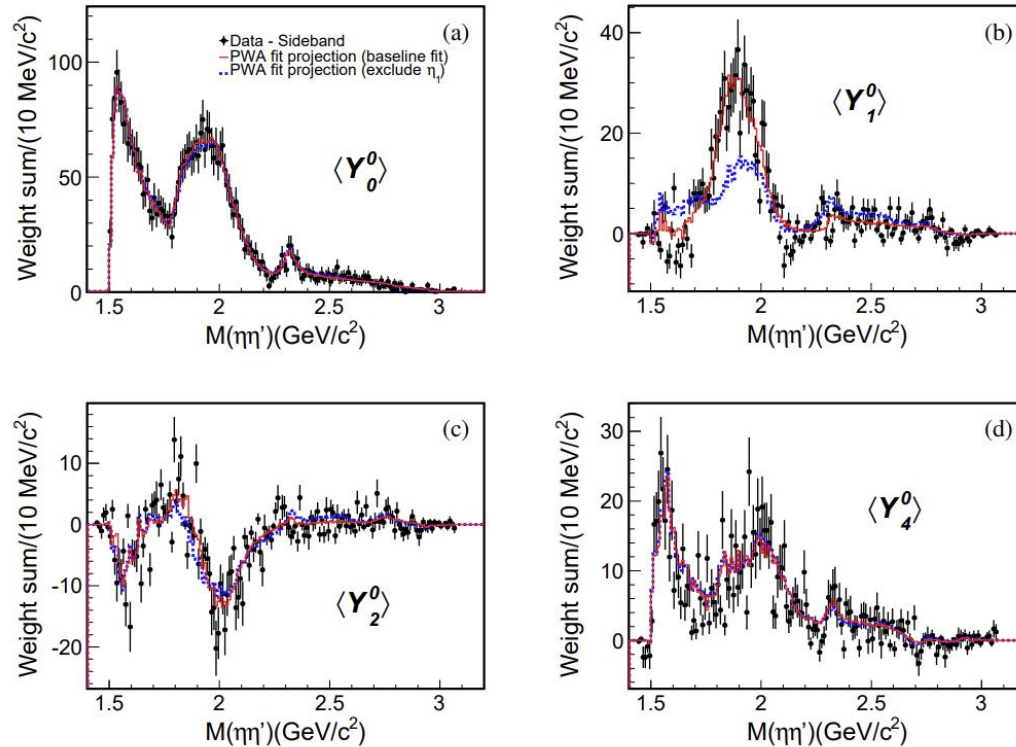


FIG. 3. The distributions of the unnormalized moments $\langle Y_L^0 \rangle$ ($L = 0, 1, 2,$ and 4) for $J/\psi \rightarrow \gamma\eta\eta'$ as functions of the $\eta\eta'$ mass. Black dots with error bars represent the background-subtracted data weighted with angular moments; the red solid lines represent the baseline fit projections; and the blue dotted lines represent the projections from a fit excluding the η_1 component.

M. Ablikim, et al., Observation of an Isoscalar Resonance with Exotic $J^{PC} = 1^{-+}$ Quantum Numbers in $J/\psi \rightarrow \gamma\eta\eta'$, Phys. Rev. Lett. 129 (19) (2022) 192002. [arXiv:2202.00621](https://arxiv.org/abs/2202.00621), [doi:10.1103/PhysRevLett.129.192002](https://doi.org/10.1103/PhysRevLett.129.192002).

$$\eta_1(1855) : M = 1855 \pm 9_{-1}^{+6} \text{ MeV}/c^2, \\ \Gamma = 188 \pm 18_{-8}^{+3} \text{ MeV}.$$



Introduction

$$\eta_1(1855) : M = 1855 \pm 9_{-1}^{+6} \text{ MeV}/c^2 ,$$
$$\Gamma = 188 \pm 18_{-8}^{+3} \text{ MeV} .$$

$$\pi_1(1400) : M = 1354 \pm 25 \text{ MeV} ,$$
$$\Gamma = 330 \pm 35 \text{ MeV} ;$$

$$\pi_1(1600) : M = 1661_{-11}^{+15} \text{ MeV} ,$$
$$\Gamma = 240 \pm 50 \text{ MeV} ;$$

$$\pi_1(2015) : M = 2014 \pm 20 \pm 16 \text{ MeV} ,$$
$$\Gamma = 230 \pm 32 \pm 73 \text{ MeV} .$$



Introduction

$$m_{\pi_1(1400)} = 1351 \pm 30\text{MeV}$$

H.-C. Kim, Y. Kim, JHEP 01 (2009) 034. arXiv:0811.0645,
doi:10.1088/1126-6708/2009/01/034.

$$m_{\pi_1(1600)} = 1980 \pm 21\text{MeV}$$

Juzheng Liang, Siyang Chen, Ying Chen, Chunjiang Shi, Wei Sun
(2024). arXiv:hep-lat/2409.14410v1.

$$m_{1^{-+}} = 2110\text{MeV}$$

C. McNeile, C. W. Bernard, T. A. DeGrand, C. E. DeTar, S. A.
Gottlieb, U. M. Heller, J. Hetrick, R. Sugar, D. Toussaint, Nucl.
Phys. B Proc. Suppl. 73 (1999) 264–266. arXiv:hep-lat/9809087,
doi:10.1016/S0920-5632(99)85043-9.



Introduction

- The QCD sum rule method has been widely applied to study the $J^{PC} = 1^{-+}$ hybrid states.

Nucl. Phys. B 248 (1984) 1–18. Phys. Lett. B 485 (2000) 145–150
Eur.Phys. J. C 8 (1999) 465–471. Z.Phys. C 34 (1987) 347.
Phys. Rev. D 76(2007) 094001. Nucl. Phys. B 196 (1982) 125–146.
Phys. Lett.B 675 (2009) 319–325.

- This method has also been applied to study the $J^{PC} = 0^{+-}$ and 2^{+-} hybrid states.

Phys. Rev. D 98 (9) (2018) 096020. Phys. Rev. D 108(2023), 114010

- The light single-gluon hybrid states with **other quantum numbers** have not been well studied in the literature. Accordingly, in this paper we shall **systematically investigate** the single-gluon hybrid states with various (exotic) quantum numbers through the QCD sum rule method.



Outline

- Introduction
- **Method of the QCD sum rules**
- Numerical analyses
- Decay behavior
- Summary

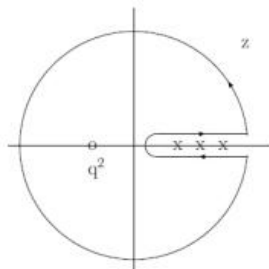
QCD sum rules

- In QCD sum rule analyses, we consider **two-point correlation functions**:

$$\begin{aligned}
 & \Pi_{1^{-+}}^{\mu\nu}(q^2) & (39) \\
 & \equiv i \int d^4x e^{iqx} \langle 0 | \mathbf{T} [J_{1^{-+}}^\mu(x) J_{1^{-+}}^{\nu\dagger}(0)] | 0 \rangle \\
 & = (g^{\mu\nu} - q^\mu q^\nu / q^2) \Pi_{1^{-+}}(q^2) + (q^\mu q^\nu / q^2) \Pi_{0^{++}}(q^2).
 \end{aligned}$$

where **J** is the current which can couple to **hadronic states**.

- We use the **dispersion relation** to express $\Pi_{1^{-+}}(q^2)$ as



The diagram shows a complex plane with a horizontal real axis and a vertical imaginary axis. A circle is drawn in the right half-plane, centered on the real axis. A point labeled q^2 is marked on the real axis to the left of the circle. A branch cut is indicated by a horizontal line starting from q^2 and extending to the right, with several 'x' marks along it. A point z is marked on the upper part of the circle.

$$\Pi_{1^{-+}}(q^2) = \int_{s_<}^{\infty} \frac{\rho_{1^{-+}}(s)}{s - q^2 - i\varepsilon} ds,$$

where $\rho_{1^{-+}}(s) \equiv \text{Im} \Pi_{1^{-+}}(s) / \pi$ is the **spectral density**, and $s_< = 4m_q^2$ is the **physical threshold**.

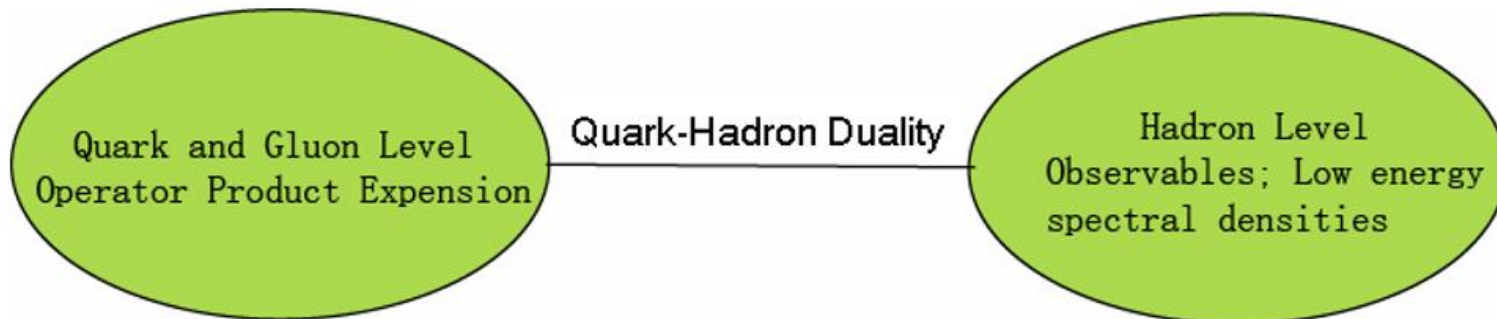
QCD sum rules

- At the **hadron level**, one pole dominance + continuum contribution:

$$\begin{aligned}
 & \rho_{1^{--}}^{\text{phen}}(s) \times (g^{\mu\nu} - q^\mu q^\nu / q^2) & (42) \\
 & \equiv \sum_n \delta(s - M_n^2) \langle 0 | J_{1^{--}}^\mu | n \rangle \langle n | J_{1^{--}}^{\nu\dagger} | 0 \rangle \\
 & = f_{1^{--}}^2 \delta(s - M_{1^{--}}^2) \times (g^{\mu\nu} - q^\mu q^\nu / q^2) + \text{continuum} .
 \end{aligned}$$

- At the **quark-gluon level**, operator product expansion (OPE). And Borel transformation at both the hadron and quark-gluon levels.

$$\begin{aligned}
 \Pi_{1^{--}}(s_0, M_B^2) & \equiv f_{1^{--}}^2 e^{-M_{1^{--}}^2 / M_B^2} \\
 & = \int_{s_0}^{\infty} e^{-s / M_B^2} \rho_{1^{--}}^{\text{OPE}}(s) ds,
 \end{aligned}$$



QCD sum rules

$$M_{1^{-+}}^2(s_0, M_B) = \frac{\int_{s_0}^{s_0} e^{-s/M_B^2} s \rho_{1^{-+}}^{\text{OPE}}(s) ds}{\int_{s_0}^{s_0} e^{-s/M_B^2} \rho_{1^{-+}}^{\text{OPE}}(s) ds}, \quad (44)$$

$$f_{1^{-+}}^2(s_0, M_B) = \Pi_{1^{-+}}(s_0, M_B^2) \times e^{M_{1^{-+}}^2/M_B^2}. \quad (45)$$

- Two parameters: M_B, s_0
- Criteria:
 1. Positivity of spectral density
 2. Convergence of OPE
 3. Sufficient amount of pole contribution
 4. The dependence of mass on parameters M_B, s_0



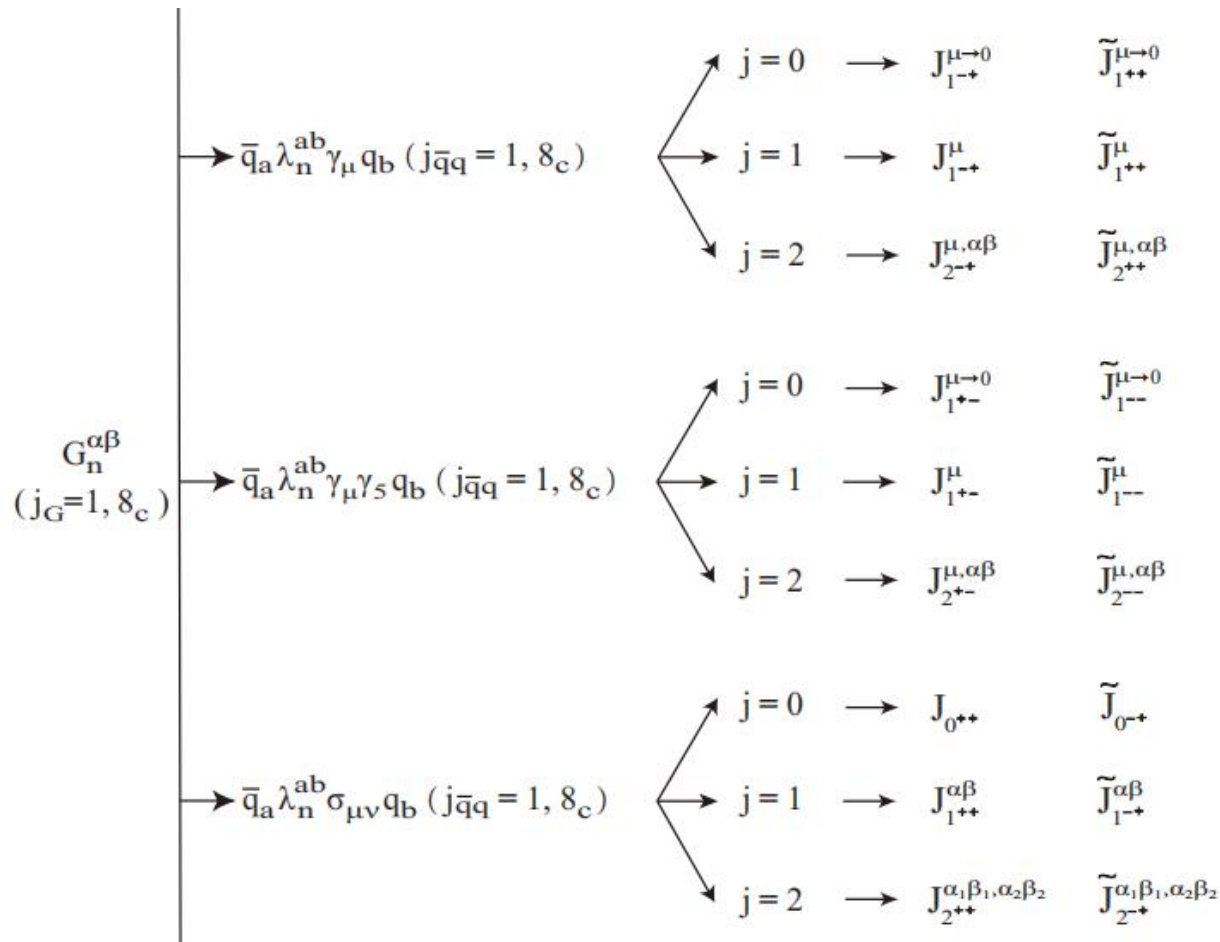
Outline

- Introduction
- Method of the QCD sum rules
- **Numerical analyses**
- Decay behavior
- Summary

Numerical analyses

Interpolating currents:

$$J_{1^{-+}}^{\mu} = \bar{q}_a \lambda_n^{ab} \gamma_{\beta} q_b g_s G_n^{\mu\beta},$$



Numerical analyses

The OPE of current J_{1-+}^μ

$$\begin{aligned} \Pi_{1-+}^\mu(M_B^2, s_0) = & \int_{4m_s^2}^{s_0} \left(\frac{s^3 \alpha_s}{60\pi^3} - \frac{m_s^2 s^2 \alpha_s}{3\pi^3} + s \left(\frac{\langle \alpha_s GG \rangle}{36\pi^2} + \frac{13 \langle \alpha_s GG \rangle \alpha_s}{432\pi^3} + \frac{8m_s \langle \bar{s}s \rangle \alpha_s}{9\pi} \right) \right. \\ & + \left. \frac{\langle g_s^3 G^3 \rangle}{32\pi^2} - \frac{3 \langle \alpha_s GG \rangle m_s^2 \alpha_s}{64\pi^3} - \frac{3m_s \langle g_s \bar{s}\sigma Gs \rangle \alpha_s}{4\pi} \right) \times e^{-s/M_B^2} ds \\ & + \left(\frac{\langle \alpha_s GG \rangle^2}{3456\pi^2} - \frac{\langle g_s^3 G^3 \rangle m_s^2}{16\pi^2} - \frac{2}{9} \langle \alpha_s GG \rangle m_s \langle \bar{s}s \rangle + \frac{11}{9} \pi \langle \bar{s}s \rangle \langle g_s \bar{s}\sigma Gs \rangle \alpha_s \right), \end{aligned}$$

The OPE with the quark-gluon content $\bar{q}qg$ ($q = u/d$) can be easily derived by replacing $m_s \rightarrow 0$, $\langle \bar{s}s \rangle \rightarrow \langle \bar{q}q \rangle$, and $\langle g_s \bar{s}\sigma Gs \rangle \rightarrow \langle g_s \bar{q}\sigma Gq \rangle$.

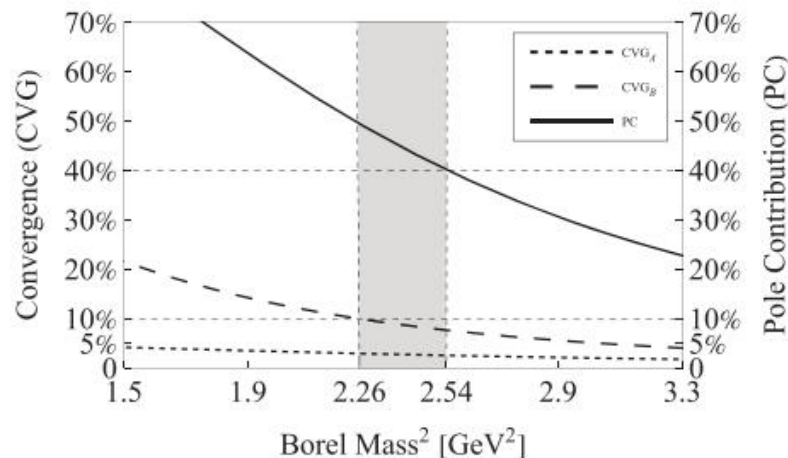
Numerical analyses

- Convergence of OPE
- Sufficient amount of pole contribution

$$\text{CVG}_A \equiv \left| \frac{\Pi^{g_s^{n=4}}(\infty, M_B^2)}{\Pi(\infty, M_B^2)} \right| \leq 5\%,$$

$$\text{CVG}_B \equiv \left| \frac{\Pi^{D=6+8}(\infty, M_B^2)}{\Pi(\infty, M_B^2)} \right| \leq 10\%.$$

$$\text{PC} \equiv \left| \frac{\Pi(s_0, M_B^2)}{\Pi(\infty, M_B^2)} \right| \geq 40\%.$$



$$2.26\text{GeV}^2 \leq M_B^2 \leq 2.54\text{GeV}^2$$

Note that this **Borel window is not so wide**, and it may indicate that the understanding of this state as a particle has **limitations**

Numerical analyses

The dependence of mass on parameters

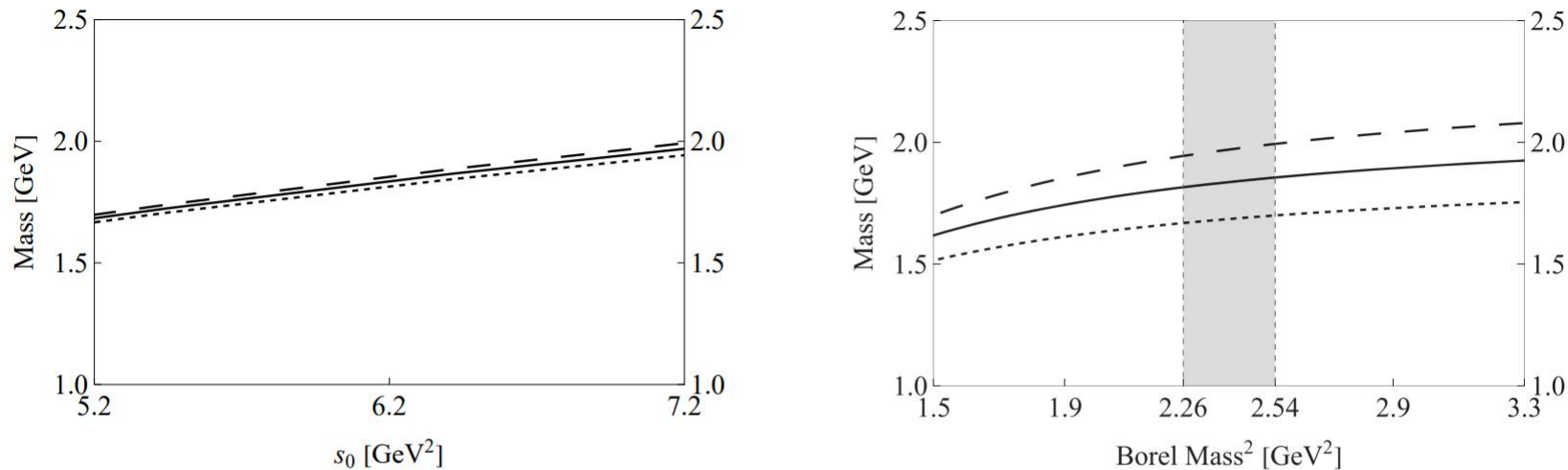


FIG. 4: Mass of the single-gluon hybrid state $|\bar{s}sg; 1^{-+}\rangle$ with respect to the threshold value s_0 (left) and the Borel mass M_B (right). In the left panel the dotted, solid, and dashed curves are obtained by setting $M_B^2 = 2.26 \text{ GeV}^2$, 2.40 GeV^2 , and 2.54 GeV^2 , respectively. In the right panel the dotted, solid, and dashed curves are obtained by setting $s_0 = 5.2 \text{ GeV}^2$, 6.2 GeV^2 , and 7.2 GeV^2 , respectively. These curves are obtained using the spectral density $\rho_{1^{-+}}^{\bar{s}sg}(s)$ extracted from the current $J_{1^{-+}}^\mu$ with the quark-gluon content $\bar{s}sg$.

$$M_{|\bar{s}sg; 0+1^{-+}\rangle} = \boxed{1.84^{+0.14}_{-0.15}} \text{ GeV}$$

Numerical analyses

Mass extracted from currents of $\bar{s}sg$

State [J^{PC}]	Current	s_0^{min} [GeV ²]	Working Regions		Pole [%]	Mass [GeV]	Decay Constant
			M_B^2 [GeV ²]	s_0 [GeV ²]			
$ \bar{s}sg; 1^{--}\rangle$	$J_{1^{--}}^{\alpha\beta}$	4.3	2.07–2.80	6.5	40–63	$1.94_{-0.21}^{+0.20}$	$0.054_{-0.016}^{+0.013}$ GeV ³
$ \bar{s}sg; 1^{+-}\rangle$	$\tilde{J}_{1^{+-}}^{\alpha\beta}$	16.2	3.60–5.40	20.0	40–65	$4.06_{-0.16}^{+0.26}$	$0.071_{-0.020}^{+0.019}$ GeV ³
$ \bar{s}sg; 1^{+-}\rangle$	$J_{1^{+-}}^{\alpha\beta}$	5.9	2.54–2.72	6.5	40–45	$2.01_{-0.20}^{+0.17}$	$0.050_{-0.006}^{+0.005}$ GeV ³
$ \bar{s}sg; 1^{--}\rangle$	$\tilde{J}_{1^{--}}^{\alpha\beta}$	16.9	3.73–5.30	20.0	40–61	$4.12_{-0.13}^{+0.26}$	$0.070_{-0.020}^{+0.019}$ GeV ³
$ \bar{s}sg; 0^{++}\rangle$	$J_{1^{+-}}^{\mu\rightarrow 0}$	20.7	5.18–7.35	26.0	40–63	$4.50_{-0.22}^{+0.23}$	$0.136_{-0.034}^{+0.030}$ GeV ³
$ \bar{s}sg; 0^{-+}\rangle$	$\tilde{J}_{1^{++}}^{\mu\rightarrow 0}$	7.2	3.45–4.08	9.5	40–53	$2.26_{-0.24}^{+0.21}$	$0.107_{-0.005}^{+0.007}$ GeV ³
$ \bar{s}sg; 0^{--}\rangle$	$J_{1^{+-}}^{\mu\rightarrow 0}$	21.6	5.36–7.23	26.0	40–59	$4.57_{-0.19}^{+0.22}$	$0.134_{-0.035}^{+0.031}$ GeV ³
$ \bar{s}sg; 0^{+-}\rangle$	$\tilde{J}_{1^{--}}^{\mu\rightarrow 0}$	7.5	3.41–3.98	9.5	40–52	$2.30_{-0.24}^{+0.20}$	$0.101_{-0.006}^{+0.007}$ GeV ³
$ \bar{s}sg; 1^{-+}\rangle$	$J_{1^{-+}}^{\mu}$	5.1	2.26–2.54	6.2	40–49	$1.84_{-0.15}^{+0.14}$	$0.300_{-0.058}^{+0.063}$ GeV ⁴
$ \bar{s}sg; 1^{++}\rangle$	$\tilde{J}_{1^{++}}^{\mu}$	14.1	3.64–4.80	17.0	40–58	$3.65_{-0.17}^{+0.17}$	$1.678_{-0.502}^{+0.530}$ GeV ⁴
$ \bar{s}sg; 1^{+-}\rangle$	$J_{1^{+-}}^{\mu}$	3.9	1.85–2.43	6.0	40–62	$1.82_{-0.15}^{+0.13}$	$0.278_{-0.056}^{+0.059}$ GeV ⁴
$ \bar{s}sg; 1^{--}\rangle$	$\tilde{J}_{1^{--}}^{\mu}$	13.8	3.50–4.80	17.0	40–61	$3.64_{-0.17}^{+0.17}$	$1.662_{-0.498}^{+0.526}$ GeV ⁴

Numerical analyses

State [J^{PC}]	Current	s_0^{min} [GeV 2]	Working Regions		Pole [%]	Mass [GeV]	Decay Constant
			M_B^2 [GeV 2]	s_0 [GeV 2]			
$ \bar{s}sg; 0^{++}\rangle$	$J_{0^{++}}$	11.5	3.53–4.33	14.0	40–55	$3.11_{-0.27}^{+0.22}$	$3.535_{-1.242}^{+1.338}$ GeV 4
$ \bar{s}sg; 0^{-+}\rangle$	$J_{0^{-+}}$	11.3	3.51–4.36	14.0	40–56	$3.08_{-0.28}^{+0.23}$	$3.509_{-1.233}^{+1.328}$ GeV 4
$ \bar{s}sg; 1^{++}\rangle$	$J_{1^{++}}^{\alpha\beta}$	6.6	1.95–2.27	7.5	40–51	$2.34_{-0.16}^{+0.14}$	$0.061_{-0.014}^{+0.012}$ GeV 3
$ \bar{s}sg; 1^{-+}\rangle$	$\tilde{J}_{1^{-+}}^{\alpha\beta}$	5.5	1.82–2.25	7.0	40–57	$2.08_{-0.24}^{+0.18}$	$0.061_{-0.010}^{+0.010}$ GeV 3
$ \bar{s}sg; 1^{-+}\rangle$	$J_{1^{-+}}^{\alpha\beta}$	5.5	1.82–2.25	7.0	40–57	$2.08_{-0.24}^{+0.18}$	$0.061_{-0.010}^{+0.010}$ GeV 3
$ \bar{s}sg; 1^{++}\rangle$	$\tilde{J}_{1^{++}}^{\alpha\beta}$	6.6	1.95–2.27	7.5	40–51	$2.34_{-0.16}^{+0.14}$	$0.061_{-0.014}^{+0.012}$ GeV 3
$ \bar{s}sg; 2^{++}\rangle$	$J_{2^{++}}^{\alpha_1\beta_1, \alpha_2\beta_2}$	9.2	3.22–3.60	10.5	40–49	$2.59_{-0.23}^{+0.19}$	–
$ \bar{s}sg; 2^{-+}\rangle$	$\tilde{J}_{2^{-+}}^{\alpha_1\beta_1, \alpha_2\beta_2}$	13.4	2.55–4.29	16.0	40–66	$3.72_{-0.13}^{+0.72}$	–
$ \bar{s}sg; 2^{-+}\rangle$	$J_{2^{-+}}^{\alpha_1\beta_1, \alpha_2\beta_2}$	8.1	3.04–3.72	10.5	40–56	$2.51_{-0.24}^{+0.20}$	–
$ \bar{s}sg; 2^{++}\rangle$	$\tilde{J}_{2^{++}}^{\alpha_1\beta_1, \alpha_2\beta_2}$	11.8	2.36–4.47	16.0	40–78	$3.54_{-0.16}^{+0.42}$	–

$$M_{|\bar{s}sg; 0+1^{-+}\rangle} = 1.84_{-0.15}^{+0.14} \text{ GeV},$$

$$f_{|\bar{s}sg; 0+1^{-+}\rangle} = 0.300_{-0.058}^{+0.063} \text{ GeV}^4$$

Numerical analyses

Mass extracted from currents of $\bar{q}qg(q = u/d)$

State [J^{PC}]	Current	s_0^{min} [GeV ²]	Working Regions		Pole [%]	Mass [GeV]	Decay Constant
			M_B^2 [GeV ²]	s_0 [GeV ²]			
$ \bar{q}qg; 1^{--}\rangle$	$J_{1^{--}}^{\alpha\beta}$	4.2	2.03–2.48	5.5	40–54	$1.80_{-0.16}^{+0.13}$	$0.051_{-0.004}^{+0.004}$ GeV ³
$ \bar{q}qg; 1^{+-}\rangle$	$\tilde{J}_{1^{+-}}^{\alpha\beta}$	16.2	3.61–4.58	18.0	40–53	$4.05_{-0.12}^{+0.24}$	$0.063_{-0.020}^{+0.020}$ GeV ³
$ \bar{q}qg; 1^{+-}\rangle$	$J_{1^{+-}}^{\alpha\beta}$	5.0	2.29–2.45	5.5	40–45	$1.84_{-0.14}^{+0.12}$	$0.049_{-0.004}^{+0.004}$ GeV ³
$ \bar{q}qg; 1^{--}\rangle$	$\tilde{J}_{1^{--}}^{\alpha\beta}$	16.3	3.52–4.56	18.0	40–53	$4.09_{-0.14}^{+0.29}$	$0.064_{-0.020}^{+0.021}$ GeV ³
$ \bar{q}qg; 0^{++}\rangle$	$J_{1^{+-}}^{\mu\rightarrow 0}$	20.6	5.11–6.59	24.0	40–56	$4.45_{-0.17}^{+0.22}$	$0.124_{-0.036}^{+0.032}$ GeV ³
$ \bar{q}qg; 0^{-+}\rangle$	$\tilde{J}_{1^{++}}^{\mu\rightarrow 0}$	7.7	3.58–3.81	8.5	40–45	$2.14_{-0.19}^{+0.17}$	$0.105_{-0.004}^{+0.005}$ GeV ³
$ \bar{q}qg; 0^{--}\rangle$	$J_{1^{+-}}^{\mu\rightarrow 0}$	21.6	5.48–6.52	24.0	40–50	$4.49_{-0.14}^{+0.21}$	$0.123_{-0.037}^{+0.032}$ GeV ³
$ \bar{q}qg; 0^{+-}\rangle$	$\tilde{J}_{1^{--}}^{\mu\rightarrow 0}$	7.1	3.32–3.73	8.5	40–49	$2.16_{-0.19}^{+0.16}$	$0.100_{-0.005}^{+0.005}$ GeV ³
$ \bar{q}qg; 1^{-+}\rangle$	$J_{1^{-+}}^{\mu}$	4.8	2.19–2.28	5.2	40–43	$1.67_{-0.17}^{+0.15}$	$0.243_{-0.052}^{+0.057}$ GeV ⁴
$ \bar{q}qg; 1^{++}\rangle$	$\tilde{J}_{1^{++}}^{\mu}$	13.8	3.59–4.10	15.0	40–48	$3.54_{-0.12}^{+0.16}$	$1.370_{-0.450}^{+0.494}$ GeV ⁴
$ \bar{q}qg; 1^{+-}\rangle$	$J_{1^{+-}}^{\mu}$	4.6	2.10–2.27	5.2	40–46	$1.68_{-0.16}^{+0.14}$	$0.242_{-0.051}^{+0.055}$ GeV ⁴
$ \bar{q}qg; 1^{--}\rangle$	$\tilde{J}_{1^{--}}^{\mu}$	13.7	3.57–4.10	15.0	40–49	$3.53_{-0.12}^{+0.16}$	$1.366_{-0.450}^{+0.493}$ GeV ⁴

Numerical analyses

State [J^{PC}]	Current	s_0^{min} [GeV ²]	Working Regions		Pole [%]	Mass [GeV]	Decay Constant
			M_B^2 [GeV ²]	s_0 [GeV ²]			
$ \bar{q}qg; 0^{++}\rangle$	$J_{0^{++}}$	11.1	3.48–3.91	12.5	40–49	$2.94_{-0.25}^{+0.20}$	$2.893_{-0.948}^{+1.029}$ GeV ⁴
$ \bar{q}qg; 0^{-+}\rangle$	$J_{0^{-+}}$	11.1	3.47–3.92	12.5	40–49	$2.93_{-0.25}^{+0.20}$	$2.882_{-0.945}^{+1.026}$ GeV ⁴
$ \bar{q}qg; 1^{++}\rangle$	$J_{1^{++}}^{\alpha\beta}$	5.8	1.84–2.06	6.5	40–48	$2.11_{-0.21}^{+0.17}$	$0.056_{-0.013}^{+0.012}$ GeV ³
$ \bar{q}qg; 1^{-+}\rangle$	$\tilde{J}_{1^{-+}}^{\alpha\beta}$	5.5	1.81–2.00	6.2	40–48	$2.00_{-0.16}^{+0.13}$	$0.055_{-0.008}^{+0.007}$ GeV ³
$ \bar{q}qg; 1^{-+}\rangle$	$J_{1^{-+}}^{\alpha\beta}$	5.5	1.81–2.00	6.2	40–48	$2.00_{-0.16}^{+0.13}$	$0.055_{-0.008}^{+0.007}$ GeV ³
$ \bar{q}qg; 1^{++}\rangle$	$\tilde{J}_{1^{++}}^{\alpha\beta}$	5.8	1.84–2.06	6.5	40–48	$2.11_{-0.21}^{+0.17}$	$0.056_{-0.013}^{+0.012}$ GeV ³
$ \bar{q}qg; 2^{++}\rangle$	$J_{2^{++}}^{\alpha_1\beta_1, \alpha_2\beta_2}$	8.6	3.11–3.37	9.5	40–46	$2.44_{-0.24}^{+0.20}$	–
$ \bar{q}qg; 2^{-+}\rangle$	$\tilde{J}_{2^{-+}}^{\alpha_1\beta_1, \alpha_2\beta_2}$	12.7	2.54–3.60	14.0	40–54	$3.68_{-0.18}^{+0.62}$	–
$ \bar{q}qg; 2^{-+}\rangle$	$J_{2^{-+}}^{\alpha_1\beta_1, \alpha_2\beta_2}$	8.3	3.07–3.41	9.5	40–48	$2.40_{-0.25}^{+0.21}$	–
$ \bar{q}qg; 2^{++}\rangle$	$\tilde{J}_{2^{++}}^{\alpha_1\beta_1, \alpha_2\beta_2}$	11.7	2.47–3.70	14.0	40–63	$3.46_{-0.11}^{+0.27}$	–

$$M_{|\bar{q}qg; 1^{-}1^{-+}\rangle} = M_{|\bar{q}qg; 0^{+}1^{-+}\rangle} = 1.67_{-0.17}^{+0.15} \text{ GeV},$$

$$f_{|\bar{q}qg; 1^{-}1^{-+}\rangle} = f_{|\bar{q}qg; 0^{+}1^{-+}\rangle} = 0.243_{-0.052}^{+0.057} \text{ GeV}^4$$



Outline

- Introduction
- Method of the QCD sum rules
- Numerical analyses
- **Decay behavior**
- Summary

Decay behavior

Decay processes: normal & abnormal

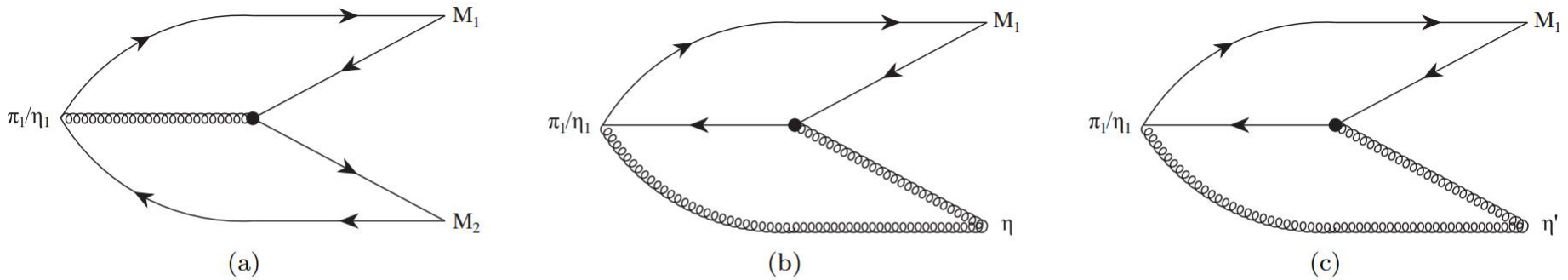


FIG. 5: Decay mechanisms of the single-gluon hybrid states through (a) the normal process with one quark-antiquark pair excited from the valence gluon, and (b,c) the abnormal processes with the η/η' produced by the QCD axial anomaly.

A. Normal decay process

three-point correlation function:

$$\pi_1 \equiv |\bar{q}qg; 1^- 1^{-+}\rangle \rightarrow \rho\pi, \quad T_{\mu\nu}(p, k, q) = \int d^4x d^4y e^{ikx} e^{iqy} \times \\ \langle 0 | \mathbb{T} [J_\nu^\rho(x) J_5^{\pi^+}(y) J_{1^{-+}}^{\mu\dagger}(0)] | 0 \rangle$$

Decay behavior

select the isovector neutral-charged one

$$J_{1^{-+}}^{\mu} \rightarrow \frac{1}{\sqrt{2}} (\bar{u}_a \lambda_n^{ab} \gamma_{\beta} u_b - \bar{d}_a \lambda_n^{ab} \gamma_{\beta} d_b) g_s G_n^{\mu\beta}$$

phenomenological side

$$T_{\mu\nu}(p, k, q) = g_{\rho\pi} \epsilon_{\mu\nu\alpha\beta} q^{\alpha} k^{\beta} \times \frac{f_{\pi_1} f_{\rho} m_{\rho} f'_{\pi}}{(m_{\pi_1}^2 - p^2)(m_{\rho}^2 - k^2)(m_{\pi}^2 - q^2)}$$

$$= -g_{\rho\pi} \frac{f_{\pi_1} f_{\rho} m_{\rho} f'_{\pi}}{m_{\rho}^2 - m_{\pi_1}^2} \left(e^{-m_{\pi_1}^2/T^2} - e^{-m_{\rho}^2/T^2} \right)$$

QCD side ➔

$$= -\frac{2\langle g\bar{q}\sigma Gq \rangle}{3\sqrt{2}} - \frac{\langle \bar{q}q \rangle \langle g_s^2 GG \rangle}{9\sqrt{2}} \frac{1}{T^2}.$$

$$T_{\mu\nu}(p, k, q) = \frac{\epsilon_{\mu\nu\alpha\beta} q^{\alpha} k^{\beta}}{q^2} \times \left(\frac{\langle g_s \bar{q} \sigma G q \rangle}{6\sqrt{2}} \left(\frac{3}{p^2} + \frac{1}{k^2} \right) - \frac{\langle \bar{q}q \rangle \langle g_s^2 GG \rangle}{18\sqrt{2}} \left(\frac{1}{p^4} + \frac{1}{k^4} \right) \right). \quad (65)$$

$$g_{\rho\pi} = 4.08_{-1.83}^{+2.40} \text{ GeV}^{-1},$$

$$\Gamma_{\pi_1 \rightarrow \rho\pi} = 242_{-179}^{+310} \text{ MeV}.$$

Decay behavior

B. Abnormal decay process

$$\eta_1 \equiv |\bar{s}s g; 0^+ 1^{-+}\rangle \rightarrow \eta\eta',$$

three-point correlation function:

$$T'_{\mu\nu}(p, k, q) = \int d^4x e^{-ikx} \langle 0 | \mathbb{T} [J_{1^{-+}}^\mu(0) J_\nu^{\eta\dagger}(x)] | \eta' \rangle, \quad J_{1^{-+}}^\mu \rightarrow \bar{s}_a \lambda_n^{ab} \gamma_\beta s_b g_s G_n^{\mu\beta}.$$

phenomenological side

$$T'_{\mu\nu}(p, k, q) = g_{\eta\eta'} k_\mu k_\nu \frac{f_{\eta_1} g_\eta}{(m_{\eta_1}^2 - p^2)(m_\eta^2 - k^2)},$$

$$g_{\eta\eta'} \frac{f_{\eta_1} g_\eta}{m_{\eta_1}^2 - m_\eta^2} \left(e^{-m_\eta^2/M_B^2} - e^{-m_{\eta_1}^2/M_B^2} \right)$$

$$= \frac{2\theta_s m_{\eta'}^2 f_{\eta'}}{3} + \frac{2\pi^2 \theta_s m_{\eta'}^2 f_{\eta'} m_s \langle \bar{s}s \rangle}{3} \frac{1}{M_B^4}.$$

QCD side

$$T'_{\mu\nu}(p, k, q)$$

$$= \theta_s k_\mu k_\nu \left(-\frac{2m_{\eta'}^2 f_{\eta'}}{3k^2} - \frac{4\pi^2 m_{\eta'}^2 f_{\eta'} m_s \langle \bar{s}s \rangle}{3k^6} \right),$$

$$g_{\eta\eta'} = 3.08_{-0.91}^{+1.30} \text{ GeV}^{-1},$$

$$\Gamma_{\eta_1 \rightarrow \eta\eta'} = 5.0_{-3.1}^{+4.6} \text{ MeV}.$$

Decay behavior

Channel	$ \bar{q}qg; 1^- 1^- +\rangle$	$ \bar{q}qg; 0^+ 1^- +\rangle$	$ \bar{s}sg; 0^+ 1^- +\rangle$
	$M = 1.67^{+0.15}_{-0.17}$ GeV	$M = 1.67^{+0.15}_{-0.17}$ GeV	$M = 1.84^{+0.14}_{-0.15}$ GeV
$\pi_1/\eta_1 \rightarrow \rho\pi$	242^{+310}_{-179}	–	–
$\pi_1/\eta_1 \rightarrow b_1(1235)\pi$	$14.5^{+25.9}_{-13.9}$	–	–
$\pi_1/\eta_1 \rightarrow f_1(1285)\pi$	$35.9^{+53.9}_{-36.4}$	–	–
$\pi_1/\eta_1 \rightarrow \eta\pi$	$2.3^{+2.5}_{-1.2}$	–	–
$\pi_1/\eta_1 \xrightarrow{b} \eta\pi$	$57.8^{+65.0}_{-31.4}$	–	–
$\pi_1/\eta_1 \rightarrow \eta'\pi$	$0.43^{+0.50}_{-0.28}$	–	–
$\pi_1/\eta_1 \xrightarrow{c} \eta'\pi$	149^{+162}_{-78}	–	–
$\pi_1/\eta_1 \rightarrow a_1(1260)\pi$	–	$79.5^{+112.4}_{-74.9}$	–
$\pi_1/\eta_1 \xrightarrow{a} \eta\eta'$	–	$0.07^{+0.12}_{-0.07}$	$0.93^{+1.04}_{-0.69}$
$\pi_1/\eta_1 \xrightarrow{b} \eta\eta'$	–	$1.62^{+2.13}_{-1.61}$	$1.64^{+1.51}_{-1.01}$
$\pi_1/\eta_1 \xrightarrow{c} \eta\eta'$	–	$11.5^{+11.7}_{-11.5}$	$5.0^{+4.6}_{-3.1}$
$\pi_1/\eta_1 \rightarrow K^*(892)\bar{K} + c.c.$	$25.3^{+34.7}_{-24.7}$	$25.3^{+34.7}_{-24.7}$	$73.9^{+85.7}_{-58.0}$
$\pi_1/\eta_1 \rightarrow K_1(1270)\bar{K} + c.c.$	–	–	$14.6^{+19.8}_{-14.6}$
$\pi_1/\eta_1 \rightarrow K^*(892)\bar{K}^*(892)$	–	–	$0.08^{+0.39}_{-0.08}$
Sum	530^{+540}_{-330}	120^{+160}_{-110}	100^{+110}_{-80}



Outline

- Introduction
- Method of the QCD sum rules
- Numerical analyses
- Decay behavior
- **Summary**

Summary

- We calculate the **masses** of forty-four single-gluon hybrid states with the quark-gluon contents $\bar{q}qg$ ($q = u/d$) and $\bar{s}sg$.
- Our results support the interpretations of the $\pi_1(1600)$ and $\eta_1(1855)$ as the hybrid states $|\bar{q}qg; 1^-1^{-+}\rangle$ and $|\bar{s}sg; 0^+1^{-+}\rangle$, respectively.
- Considering the **uncertainties**, our results suggest that the $\pi_1(1600)$ and $\eta_1(1855)$ may also be interpreted as the hybrid states $|\bar{q}qg; 1^-1^{-+}\rangle$ and $|\bar{q}qg; 0^+1^{-+}\rangle$, respectively.
- To differentiate these two assignments and to verify whether they are hybrid states or not, we propose to examine the $a_1(1260)\pi$ decay channel in future experiments.

Thanks for your attention !